



City Research Online

City, University of London Institutional Repository

Citation: Mejía-Mejía, E., Budidha, K., Kyriacou, P. A. & Mamouei, M. H. (2022). Comparison of pulse rate variability and morphological features of photoplethysmograms in estimation of blood pressure. *Biomedical Signal Processing and Control*, 78, 103968. doi: 10.1016/j.bspc.2022.103968

This is the published version of the paper.

This version of the publication may differ from the final published version.

Permanent repository link: <https://openaccess.city.ac.uk/id/eprint/29120/>

Link to published version: <https://doi.org/10.1016/j.bspc.2022.103968>

Copyright: City Research Online aims to make research outputs of City, University of London available to a wider audience. Copyright and Moral Rights remain with the author(s) and/or copyright holders. URLs from City Research Online may be freely distributed and linked to.

Reuse: Copies of full items can be used for personal research or study, educational, or not-for-profit purposes without prior permission or charge. Provided that the authors, title and full bibliographic details are credited, a hyperlink and/or URL is given for the original metadata page and the content is not changed in any way.

City Research Online:

<http://openaccess.city.ac.uk/>

publications@city.ac.uk



Comparison of pulse rate variability and morphological features of photoplethysmograms in estimation of blood pressure

Elisa Mejía-Mejía^a, Karthik Budidha^b, Panayiotis A. Kyriacou^{a,b}, Mohammad Mamouei^{b,*}

^a Research Centre for Biomedical Engineering, City, University of London, London, United Kingdom

^b Pleth Allytics Ltd, Hatfield, United Kingdom

ARTICLE INFO

Keywords:

Photoplethysmography
Pulse rate variability
Blood pressure
Features
Machine learning

ABSTRACT

Photoplethysmography is an optical technique that produces a wealth of information about cardiovascular health. Therefore, the technology has become an integral part of personal health monitoring devices. Given the importance of blood pressure measurement and control in physical and mental health, in recent years, the estimation of blood pressure from photoplethysmography has been an active area of research with promising results. Most studies on the subject rely on the morphological features of the photoplethysmogram. These features are highly prone to noise, changes in sensor placement, and skin properties; including skin colour. To address these limitations, we investigated the feasibility of using pulse rate variability features which are known to be less prone to the aforementioned limitations. To this end, we collected high quality photoplethysmograms using a bespoke, research-grade device from 18 healthy subjects. Approximately 15 min of photoplethysmograms and continuous blood pressure waveforms were collected from each subject. We trained machine learning models based on different feature sets and compared their performances. The model with morphological features alone outperformed the model with pulse rate variability features, root mean squared error (RMSE) of 6.32 vs 7.23 mmHg. However, the best performance was obtained using the combined set of features (RMSE: 5.71 mmHg). Combined, the evidence shows that the estimation of BP from PRV, alone or in conjunction with morphological features, is feasible. In light of the limitations of morphological features in estimation of blood pressure, our findings lend support to further research on the use of pulse rate variability features.

1. Introduction

Blood pressure (BP) is considered one of the most important markers of cardiovascular health and predictors of cardiovascular diseases [1, 2]. Monitoring systolic and diastolic blood pressure both in clinical and non-clinical environments, is globally recognised as an efficient and cost-effective strategy in prevention and management of several pathological conditions [3,4].

Healthy BP values are considered to be between 90 and 120 mmHg for systolic blood pressure, and 60 and 80 mmHg for diastolic blood pressure [2]. Chronically high blood pressure values above 120/80 mmHg, known as hypertension, or chronically low values, below 90/60 mmHg, known as hypotension, may negatively impact the flow of blood to tissues and, as a consequence, cardiovascular homeostasis [1, 2]. A more granular classification, that informs treatment and monitoring options for different levels of blood pressure values is provided by the American Heart Association and is presented in Table 1 [5].

Both hypertension and hypotension are abnormal conditions that should be regularly monitored for detection, prevention and treatment

of related diseases [3]. However, measuring BP values in a continuous and reliable way is still a challenge. Continuous BP measurement with clinical-grade accuracy can be obtained using invasive methods namely catheters. This can only be performed in clinical settings and increases the risk of infection [3]. A common, indirect and noninvasive approach is the oscillometric technique, which is based on the inflation of a cuff. This does not allow for continuous measurements and could be cumbersome and impractical in some settings, such as in sleep studies [6,7].

Several approaches towards continuous, non-invasive measurement of BP have been pursued in recent decades [8–10]. One technique that has been largely studied for BP estimation is photoplethysmography (PPG) [3,9,11]. PPG is a noninvasive, optical technique that reflects blood volume changes in peripheral tissue [12]. Due to its simplicity and low-cost PPG is nowadays widely used, especially in wearable devices, for the monitoring of vital signs such as pulse rate and blood oxygen saturation. PPG has also received much attention for the estimation and assessment of other variables, such as arterial stiffness, blood

* Corresponding author.

E-mail address: m.mamouei@plethai.com (M. Mamouei).

<https://doi.org/10.1016/j.bspc.2022.103968>

Received 3 March 2022; Received in revised form 18 June 2022; Accepted 11 July 2022

Available online 6 August 2022

1746-8094/© 2022 The Author(s). Published by Elsevier Ltd. This is an open access article under the CC BY license (<http://creativecommons.org/licenses/by/4.0/>).

Table 1

Classification of blood pressure values according to the American Heart Association [5].

Blood pressure category	SBP (mmHg)	DBP (mmHg)	Condition
Normal	< 120	< 80	Both SBP and DBP
Elevated	120 – 129	< 80	Both SBP and DBP
Hypertension Stage 1	130 – 139	80 – 89	Either SBP or DBP
Hypertension Stage 2	> 140	> 90	Either SBP or DBP
Hypertensive crisis	> 180	> 120	Either SBP or DBP

SBP: Systolic blood pressure; DBP: Diastolic blood pressure.

Table 2

Comparison of results found in the literature for the estimation of BP using pulse rate variability (PRV) features from data obtained from the MIMIC database. SBP: Systolic blood pressure. DBP: Diastolic blood pressure. MAP: Mean arterial pressure.

Study	Mean absolute error (mmHg)		
	SBP	DBP	MAP
Slapničar et al. [21]	4.47	2.02	–
Slapničar et al. [22]	9.43	6.88	–
Leitner et al. [23]	3.43	1.73	–
Athaya and Choi [24]	3.68 ± 4.42	1.97 ± 2.92	2.17 ± 3.06
Aguirre et al. [25]	14.39 ± 0.42	6.57 ± 0.20	8.89 ± 0.10
Mejía-Mejía et al. [15]	4.74 ± 2.33	1.78 ± 0.14	2.55 ± 0.78

pressure and pulse rate variability (PRV) [13]. PRV describes changes in pulse rate overtime, which has been used as an indirect marker of the cardiovascular autonomic activity [13,14] and has also been found to correlate with blood pressure [15,16].

Most of the proposed techniques for the estimation of BP from PPG signals are based on machine learning (ML) algorithms and the use of morphological features of the PPG [3,4]. These features are highly sensitive to external factors that affect the shape of the signal such as noise, motion artefacts, sensor placement and the composition of the skin including melanin content (i.e. skin colour). On the contrary PRV features are (a) easier to detect, therefore less prone to noise, and (b) are independent of skin properties. Therefore, the use of PRV features in the estimation of BP may improve the accuracy of predictions and mitigate some of the aforementioned limitation. However, it is first important to evaluate whether accurate estimation of BP from PRV in healthy individuals is feasible.

Previous studies have aimed to use PPG and PRV to estimate BP values. Gaurav et al. extracted PRV- and PPG-based features from PPG signals and estimated systolic and diastolic blood pressure using artificial neural networks, reaching mean absolute errors of 4.47 and 3.21 mmHg [17]. Kei-Fong et al. obtained PPG signals using a multi-sensor system located at the wrist, and extracted PRV, PPG and PTT features in order to estimate BP values using support vector machines, finding a mean absolute error of 7.29 ± 5.3 mmHg for SBP, and 5.01 ± 4.1 mmHg for DBP [18]. Similarly, Mejía-Mejía et al. [15] recently used machine learning algorithms and solely PRV features for BP estimation, and found comparable results with data obtained from the MIMIC database [19,20], which have been used by several authors for the estimation of blood pressure from PRV and PPG. Table 2 summarises some of these results.

The accuracy of BP estimation is undoubtedly important, but robustness to noise and mitigation of sensitivity to skin properties are equally crucial for practical applications. In light of this, PRV-based features have advantages compare to morphological features, but a comprehensive comparison of the two approaches in healthy subjects is missing from the literature. In this study, our primary objective is to evaluate the predictive value of PRV features (hereafter denoted by PRV) relative to morphological features (hereafter denoted by PPG) and the combined set of features (hereafter denoted by PPG+PRV) to shed light on their independent information and complementarity for BP estimation. To ensure the quality of morphological features are not deteriorated due to signal quality and noise we used a custom-made, research-grade device, BioBlocks™ and carried out the study on a group of healthy individuals at rest. The main contribution of this study is

to investigate the interplay and complementarity of PRV- and PPG-based features for BP estimation. We performed the comparison using a custom-made, research-grade device that ensure high SNR and we trained various ML models to ensure the findings are independent of the complexity of models.

2. Materials and methods

2.1. Signal acquisition

Photoplethysmographic (PPG) and continuous arterial blood pressure (ABP) signals were simultaneously acquired from 20 healthy volunteers (12 men, 34 ± 5 years old; 8 women, 32 ± 4 years old). Subjects with cardiovascular, pulmonary, or metabolic diseases were excluded from this study. The study was explained to the subjects before data acquisition and they all gave informed consent regarding their participation in this study.

All subjects were seated on a comfortable chair, with their hands approximately at heart level. Infrared PPG signals were acquired from the index finger of each subject, using a 50 custom-made, research-grade PPG acquisition system, BioBlocks™ (Pleth ALLytics Ltd, United Kingdom). Continuous ABP wave were simultaneously acquired using a CNAP Monitor (CN Systems, Austria) with the sensor located on the middle and ring fingers of the same hand as the PPG probe. The CNAP monitor is based on the Vascular Unloading Technique and utilises a dual finger probe for a beat-to-beat measurement of ABP [26]. Both PPG and BP signals were digitised and 55 acquired using a Data Acquisition Card (National Instruments, United States) and a Virtual Instrument developed in LabVIEW™ (National Instruments, United States). Fig. 1 shows the acquisition setup. Signals were acquired for approximately 15 min with a sampling rate of 1 kHz, and stored for offline processing, which was performed in MATLAB R2019b (Mathworks, United States) and Python 3.8.5.

2.2. Arterial blood pressure analysis

Fig. 2 summarises the processing of arterial blood pressure (ABP) and PPG signals for the extraction of BP information using PRV and morphological PPG features. ABP signals were segmented into 2-minute segments with the stride length of 10 s (an overlap of 110 s). Shorter segment lengths led to very poor predictions and longer window lengths would have undesired implications for practical applications. Once segmented, each ABP signal portion was filtered using a 50th-order moving-average filter and calibrated using (Eq. (1)), where



Fig. 1. Setup for the simultaneous acquisition of photoplethysmographic signals and continuous arterial blood pressure.

X_{Volts} is the measured signal, in Volts, and X_{mmHg} is the calibrated pressure signal in pressure units (mmHg). This calibration equation was determined as suggested for the CNAP Monitor.

$$X_{mmHg} = 50 + 100 \frac{X_{Volts} - 0.0703}{0.1683 - 0.0703} \quad (1)$$

Peaks and onsets were detected from the calibrated pressure signals using the algorithm described in [27]. This algorithm is based on the first derivative of the pulsatile signal and the use of adaptive thresholds based on a low-pass filtered version of the signal. From the first derivative of the signal, zero-crossings are detected and beat locations are determined according to the estimated thresholds and the detected zero-crossings. Then, peaks and onsets are detected from each beat. Then, these points were interpolated using a cubic spline interpolation, to obtain an estimated trend for the systolic (SBP) and diastolic blood pressures (DBP). The mean values of these trends were then obtained for each ABP segment. Given the clinical importance of SBP, for conciseness, the rest of the analysis focuses on the prediction of SBP.

2.3. Photoplethysmographic signals processing

Fig. 2 illustrates the processing of PPG signals for the extraction of BP values from PPG signals.

2.3.1. Pre-processing of signals

Similar to ABP signals, PPG signals were segmented into 2-minute segments with a 10-second stride between consecutive segments. The segmented PPG signals were then filtered using a second order Butterworth band pass filter, with cut-off frequencies of 0.5 and 12 Hz.

2.3.2. Segmentation of interbeat intervals

Inter-beat intervals (IBIs) were extracted from the PPG segments applying the algorithm D2Max, described in [28]. This algorithm detects peaks from the second derivative of the PPG signal. For the detection of the cardiac cycles, each 2-minute PPG segment was detrended and further filtered using a band pass, second order Butterworth filter with cut-off frequencies of 0.5 and 10 Hz. Then, the D2Max algorithm was applied to each 10-second PPG segment. Once the cycles in each

10-second segment were detected, they were corrected based on the length of the cycles. Those fiducial points related to cycles shorter than physiologically expected were deleted, while additional fiducial points were added in those IBIs that were longer than expected.

From the extracted IBIs, PRV trends were obtained from the duration of IBIs for the subsequent extraction of PRV-related features. Outliers from these trends were detected as those IBIs with duration lower than the average duration of IBIs minus 1.96 times their standard deviation, or with duration higher than the average plus 1.96 times their standard deviation. An interpolated trend was also obtained for the assessment of frequency-related information, using a cubic spline interpolation with sampling rate of 4 Hz.

2.3.3. Feature extraction

Time and frequency domain, and non-linear indices were extracted from the 2-minute PRV trends. In the time domain, indices extracted were the average duration of IBIs (denoted by AVNN), their standard deviation (SDNN), the root-mean squared value of successive difference of IBIs (RMSSD), and the value and proportion of successive differences longer than 50 [ms] (NN50 and pNN50). Frequency spectra was assessed using the fast Fourier transform (FFT) of the detrended IBIs, calculated with 4096 samples after zero-padding, to get a frequency resolution of approximately 0.001 Hz. From these spectra, the very-low (VLF, $f \geq 0.0033$ and $f \leq 0.04$ Hz), low (LF, $f > 0.04$ and $f \leq 0.15$ Hz) and high-frequency (HF, $f > 0.15$ and $f \leq 0.40$ Hz) bands were extracted as the area under the curve, as well as the total power (TP) of the spectrum between 0.0033 and 0.40 Hz. Normalised power of the LF and HF bands (nLF and nHF, respectively) were also measured, as well as the ratio between LF and HF (LF/HF). Similarly, the x- and y-coordinates of the centroid of the LF (cLFx and cLFy), HF (cHFx and cHFy) and TP (cTPx and cTPy) bands were obtained. Finally, the spectral entropy (SpEn) from the spectrum was assessed.

Non-linear indices were also obtained from the PRV trends. Poincaré plot indices based on the ellipse-fitting technique were measured, extracting the area of the ellipse (S), its major and minor diameters (SD1 and SD2), the ratio between diameters (SD1/SD2), and the compaction of the ellipse (COM). Detrended-fluctuation analysis was also performed, and the first two scaling exponents, α_1 and α_2 were extracted. Entropy analyses were performed, and basic-scale entropy

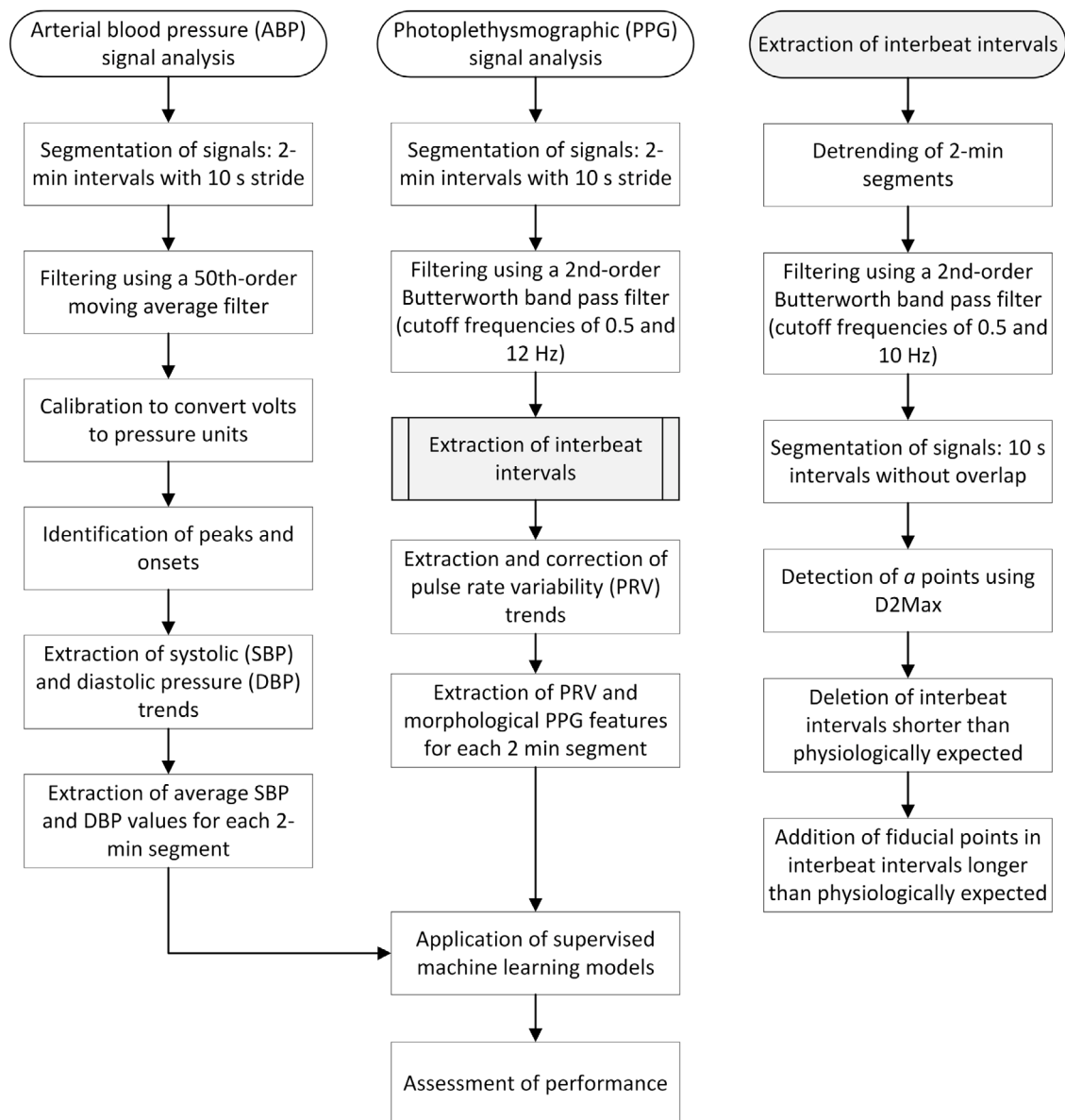


Fig. 2. Block diagram of the processing of arterial blood pressure (ABP) and photoplethysmographic (PPG) signals for the estimation of blood pressure (BP) using machine learning and morphological PPG and pulse rate variability (PRV) features.

(BSE), sign-series entropy (SSE), approximate entropy (ApEn), sample entropy (SampEn) and multi-scale entropy (MSE) were measured. Additionally, automutual information (AMIF) analysis was performed, and the lag of τ (LagT), the lag of the first peak (LagPD) and the value of the AMIF curve at the first peak (PD) were derived. Finally, the correlation dimension (D2), the maximum Lyapunov exponents (LYA) and the embedded dimension of the nonlinear model that approximates the phase of the PRV trend (EMBDIM) were assessed. Further information regarding the extraction of these indices can be found in [15].

From the PPG cardiac cycles and its derivatives, morphological features were extracted, and then the mean, standard deviation, median and interquartile range of these features were assessed for each 2-minute PPG segment. For each cardiac cycle, the initial and final onsets were obtained and used as reference to obtain other fiducial points from the PPG. A total of 478 features were extracted from each segment. Some of these features are illustrated in Fig. 3 1. A description of all the extracted morphological features is included in the supplementary material (Tables A.1 and A.2).

2.4. Estimation of blood pressure values

Using PRV features, PPG features and the combination of both, machine learning models were trained to automatically estimate the systolic blood pressure. Two types of models were generated, a gradient boosting regressor (XGBR) and a support vector regressor (SVR). All data features were normalised, by setting the mean equal to zero and standard deviation equal to one. To limit the effects of possible outliers, all values below -5 and above 5 were clipped to -5 and 5 , respectively. Models were trained with the first 12 min of signals from each participant (corresponding to 60 overlapping segments). The remaining segments which in average had 3 min of data were used as test set. Note segment 72 onwards were used as the test set to ensure no overlap between the training and test sets. For the XGBR models, to avoid overfitting we selected a non-overlapping validation set for early stopping. To this end, the training set was further split into training set (segments 1 to 40) and validation set (segments 52 to 60). Models were fitted using a Bayesian Hyperparameter tuning with five-fold cross validation.

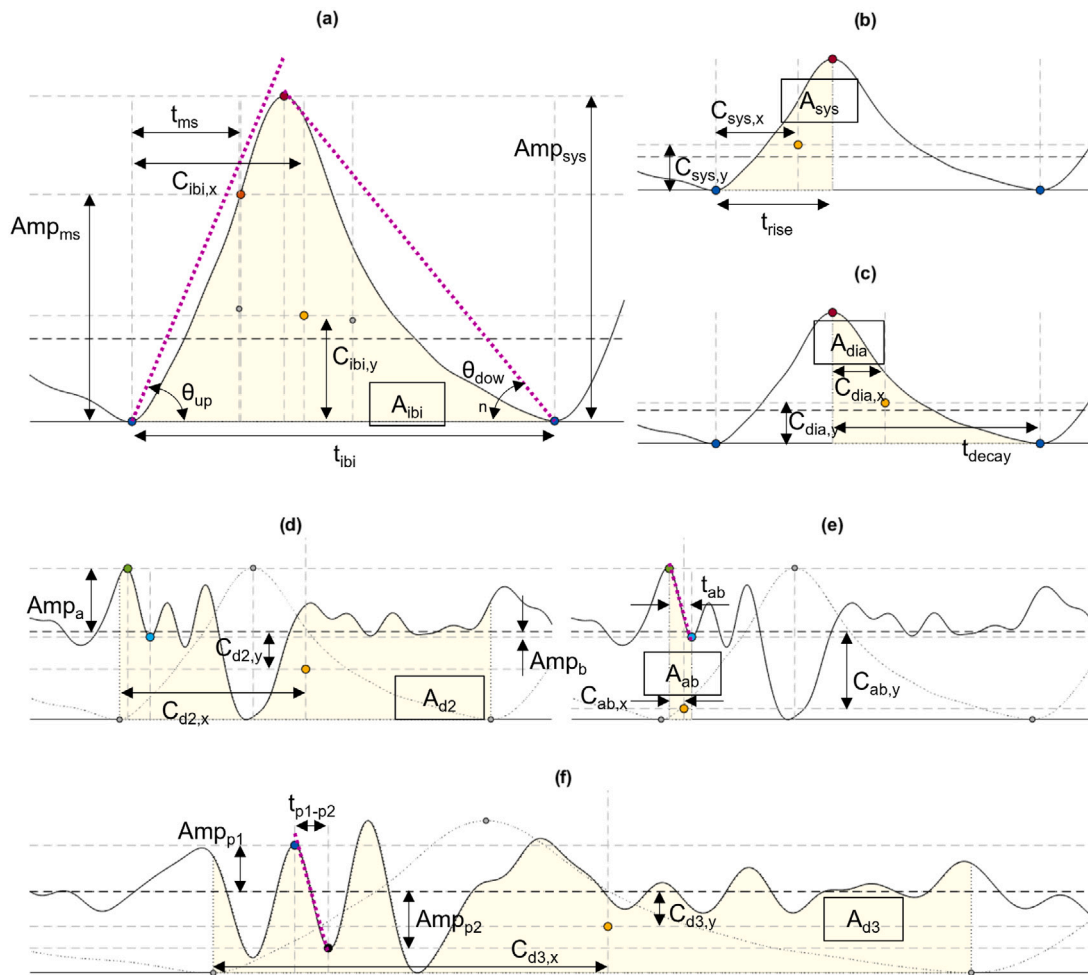


Fig. 3. Example of some of the features extracted from the photoplethysmographic (PPG) cardiac cycles (a), its first derivative, and its systolic (b) and diastolic (c) phases; the second derivative of the PPG cardiac cycle (d and e); and the third derivative of the PPG cardiac cycle (f).

The hyperparameters for each model were uniformly sampled from the options shown in Appendix B.

2.5. Performance assessment

The performance of the resulting models was assessed using the root-mean squared error between expected and estimated blood pressure values, and by generating Bland-Altman plots to understand the agreement between the predicted and real values. Since three models were generated in each case, i.e. a model using only PRV indices, another model using only PPG features, and one using the combination of both types of features, the performance of these models were compared using an analysis of variance, to evaluate if using both PRV and PPG features results in a better performance from the algorithms.

3. Results

3.1. Signals processing and feature extraction

Fig. 4 shows an example of the ABP and PPG signals used in this study. As explained, the mean, systolic and diastolic blood pressure values were extracted from each 2-minute ABP segment. Table 3 summarises the values measured from each subject. Given that most of the subjects were normotensive, subjects 4 and 10 were discarded for subsequent analyses. Tables C.1 to C.3 in the Supplementary Material show the summary of the extracted features.

3.2. Estimation of blood pressure

Using the extracted features, XGBR and SVR models were trained for the regression of blood pressure values using only PRV, only PPG and both types of features. The hyperparameters for the models can be found in supplementary materials (Table B.2). Table 4 presents the RMSE values obtained with the test dataset with each of the models.

Fig. 5 shows the scatter plots of the predicted blood pressure values against the reference values. In this figure, we used nonparametric locally weighted scatterplot smoothing (LOWESS) with bootstrapping to obtain 95% bootstrap confidence intervals [29]. The corresponding Bland Altman plots are included in the supplementary material (Figure D.1).

Lastly to evaluate whether the observed difference in predictive performance are statistically significant, we performed analysis of variance (ANOVA) on prediction errors of different models, i.e. XGBR or SVR with different feature sets. There were no statistically significant differences between the XGBR models with the three feature sets (p -value = 0.139) while the difference between the performance of the SVR models was significant (p -value < 0.001). A post-hoc analysis (Tukey's honest significant difference test), confirmed the higher accuracy of the SVR model with the morphological features relative to PRV features but did not show a significant difference between the morphological features and the combined feature set (for details see Table D.1 and Figure D.2 in the Supplementary Material).

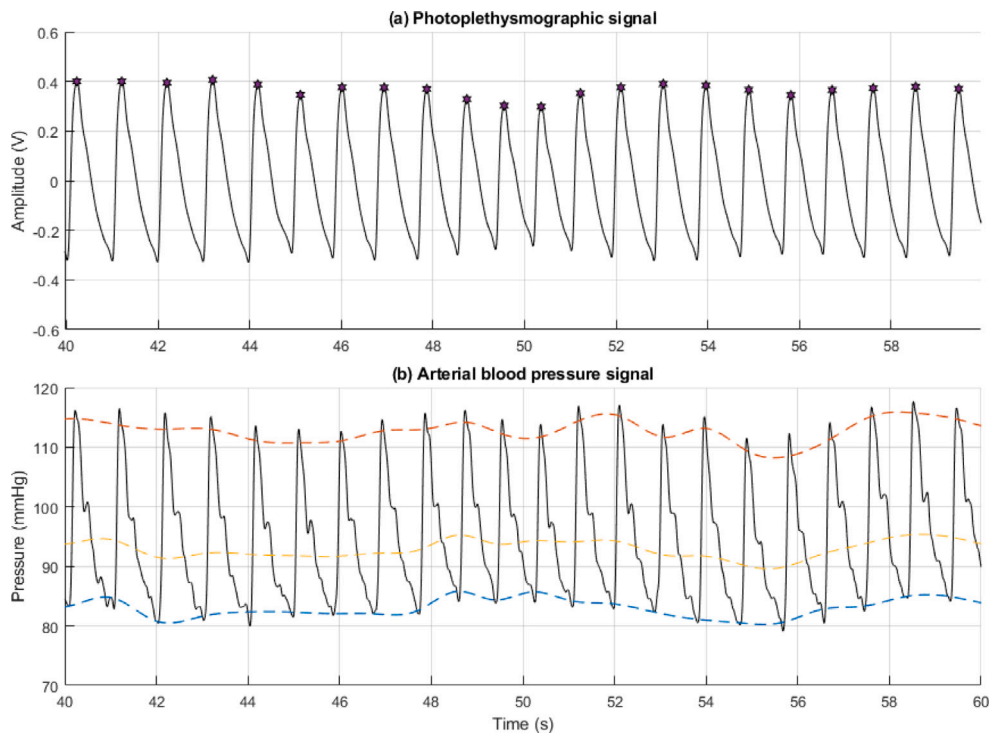


Fig. 4. Example of acquired (a) photoplethysmographic (PPG), and (b) arterial blood pressure (ABP) signals. The purple dots indicate the detection of the cardiac cycles from the PPG signal, while the discontinuous orange, yellow and blue lines represent the systolic, mean and diastolic blood pressure trends.

Table 3

Summary (mean \pm standard deviation) of blood pressure values, in mmHg, measured from arterial blood pressure signals.

Subject	Systolic blood pressure	Diastolic blood pressure	Mean arterial pressure
1	122.78 \pm 1.56	67.66 \pm 1.23	86.03 \pm 0.86
2	138.87 \pm 1.02	95.00 \pm 1.86	109.62 \pm 1.39
3	155.68 \pm 2.58	98.65 \pm 0.68	117.66 \pm 1.14
4	227.09 \pm 18.94	114.58 \pm 11.82	152.09 \pm 13.03
5	107.67 \pm 0.90	67.02 \pm 1.17	80.57 \pm 1.06
6	132.63 \pm 1.73	91.08 \pm 1.49	104.93 \pm 1.33
7	126.12 \pm 1.57	85.49 \pm 1.62	99.03 \pm 1.41
8	153.06 \pm 2.36	91.14 \pm 0.85	111.78 \pm 1.00
9	113.02 \pm 1.65	82.46 \pm 1.14	92.64 \pm 1.27
10	163.63 \pm 1.08	90.50 \pm 1.88	114.88 \pm 1.53
11	125.54 \pm 1.29	90.30 \pm 0.67	102.04 \pm 0.58
12	129.88 \pm 3.90	87.89 \pm 2.86	101.89 \pm 3.20
13	118.02 \pm 12.31	56.36 \pm 5.03	76.92 \pm 6.70
14	101.64 \pm 1.88	70.03 \pm 2.06	80.57 \pm 1.99
15	131.51 \pm 1.97	89.85 \pm 1.93	103.73 \pm 1.81
16	123.90 \pm 1.67	68.61 \pm 0.93	87.04 \pm 0.87
17	130.34 \pm 1.35	81.39 \pm 1.02	97.71 \pm 1.09
18	116.06 \pm 1.11	82.31 \pm 1.65	93.56 \pm 1.09
19	112.89 \pm 1.40	68.63 \pm 1.07	83.38 \pm 0.88
20	109.38 \pm 1.05	68.53 \pm 1.18	82.15 \pm 0.98
All	132.13 \pm 27.69	82.46 \pm 13.99	99.02 \pm 17.56

MAP: Mean arterial pressure.

SBP: Systolic blood pressure.

DBP: Diastolic blood pressure.

Table 4

Root-mean square errors, in mmHg, obtained from the trained models using the test dataset. PRV: Pulse rate variability. PPG: Photoplethysmography.

Features	Gradient booster regressor	Support vector regression
PRV	9.12	10.01
PPG	7.86	6.32
PRV + PPG	7.22	5.71

4. Discussion

Continuous, non-invasive blood pressure estimation has gained increasing attention in recent years due to the high levels of cardiovascular-related issues around the world [3,15]. Due to its widespread use both in clinical and everyday scenarios, and its relationship with blood flow and volume, PPG has been proposed as one of the most promising techniques for ubiquitous, reliable measurement of blood pressure values, which could enhance the diagnosis and monitoring of live threatening conditions such as hypertension and diabetes.

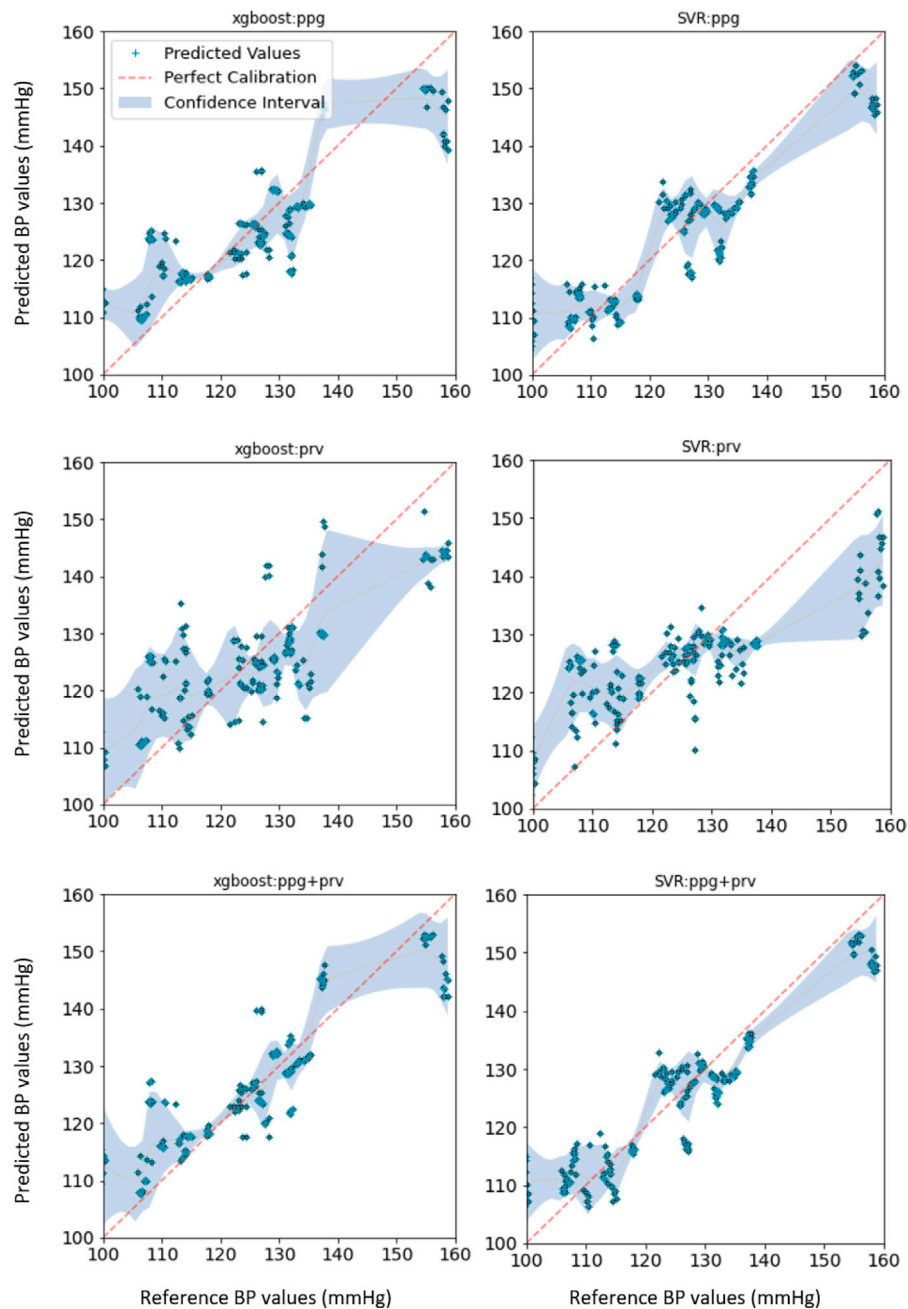


Fig. 5. Scatter plots of the predicted blood pressure values against the reference values for different models.

Although promising, some of the studies found in the literature make use of very complex techniques for the extraction of PPG features or for the learning algorithms, which limit their application in real-life scenarios. The aim of this study was to investigate the predictive performance of morphological features from the PPG against PPG-based PRV features, for the estimation of systolic blood pressure values using two well-known machine learning techniques, i.e. XGBoost and SVR.

Features from PRV and PPG morphology were extracted in this analysis. PRV, which describes the variability of pulse rate through time, is an indirect marker of autonomic activity and has been proposed as a surrogate of heart rate variability in healthy, young, resting subjects [13]. In a beat-to-beat basis, blood pressure is primarily regulated by the sympathoadrenal system [2], and the association between PRV and changes in pulse transit time, i.e. the time between the transition of the pulse wave from the heart to the peripheral tissue [30,31]. Therefore, Mejía-Mejía et al. proposed the estimation of blood pressure

values using PRV-based features, with relatively good performance in critically-ill subjects [15]. In this study, the same features proposed in this previous work were extracted from 2 min PPG segments. Similarly, several studies have proposed the extraction of morphological features from the PPG signal [3]. In this study, several of the features reported in the literature [32] were used for the characterisation of 2-minute PPG signals. Since the extraction of these features was based on the morphology of each beat, they were summarised using the mean, median, standard deviation and interquartile range values.

All the features extracted for this study have been thought to be simple features to extract in a real-time basis, and do not require high computational power, so they could be extracted using embedded systems. However, they are all based on the segmentation of the cardiac cycles from the PPG signal. Several algorithms for the detection of cardiac beats from PPG signals have been proposed in the literature, with varying success and advantages for each [32]. In this study, we

used the algorithm proposed by Elgendi et al. [28], since it was found to perform better for the determination of PRV indices when compared to other algorithms proposed in the literature [33]. Moreover, Butterworth filters were applied to process the PPG signals, given their good performance in the extraction of PRV features as well as their flat pass band compared to other infinite-impulse response filters [34]. However, this filter has a non-linear phase, which could affect the shape of the PPG signal and hence the extracted morphological features. Future studies should aim to understand how this filtering process affect the estimation of morphological features from the PPG, and to standardise the use of specific filters for extracting this kind of information from these signals.

The primary goal of this study was to compare the performance of PRV and morphological features in prediction of blood pressure in healthy individuals. The use of morphological features for this purpose has been extensively studied in the literature but the sensitivity of morphological features to the quality of signal, noise, sensor placement and skin properties are some the limitations of this approach. PRV features can address these limitations but their use in healthy subjects was not explored before. The results highlighted that PRV-based estimation of BP in healthy subjects is feasible, albeit with a lower accuracy relative to morphological features. The model that combined all features delivered a higher predictive performance relative to the model with morphological features alone, although this difference was not statistically significant.

One of the main advantages of the proposed methodology, alongside the use of robust features obtained from PRV and the morphology of the PPG, is the fact that there is no need of a previous calibration for each subject, which is usually needed in these kind of approaches, especially those based on pulse wave velocity analysis [35]. Removing the need for calibration allows for an immediate and seamless use of a BP measurement device for assessing blood pressure without the need of having it adapted to each subject or to have it re-calibrated every certain time, making it more reliable for wearable and everyday devices.

These finding should be interpreted in light of the study design and its limitations. We used a bespoke, research-grade signal acquisition device to ensure the signals have a high quality. Moreover, the signals were obtained in a noise-free setting. These settings are optimal for BP estimation based on morphological features; therefore, the results are not reflective of the benefits of the two approaches in practical scenarios. Similar analysis of the comparison of the two approaches, in practical scenarios and across different skin types an important topic for future investigations.

4.1. Limitations of the study

This study has several limitations. First, data used was obtained from a small number of healthy subjects which limits the generalisability of the findings and hinders a subject-independent approach. Moreover, given the limited variability of BP in the subjects, the findings do not reflect the capacity of the models to extrapolate. Future studies should aim to obtain a larger and more heterogeneous dataset for the validation of the model, and control for gender bias. Also, features used in this study depend on the cardiac beat segmentation from the PPG signal, which could increase the complexity and error in the framework, specially for data obtain from unhealthy subjects. Other features that do not rely on the segmentation of cardiac beats could modify and improve the behaviour of machine learning models for BP estimation, hence future studies should evaluate the performance of models using these features and data acquired from a wider population. Lastly, we did not apply feature selection. This could improve both the predictive performance and computational requirements, but this was beyond the scope of the present investigation. The next step in this investigation should consider selecting the better performing combination of features for BP estimation using both morphological and PRV features.

5. Conclusion

Blood pressure estimation in a continuous, non-invasive manner has gained much attention in recent decades due to the relationship of this vital sign to general well-being and cardiometabolic health. The increasing burden of chronic and acute diseases such as diabetes and heart failure call for novel and effective strategies in monitoring and management of hypertension. The ability to measure blood pressure using an affordable and accessible signal like PPG presents an important opportunity to improve the monitoring and early detection of various conditions. However, the limitations of the current approaches, specifically, sensitivity to noise, sensor placement, and skin properties could hamper their adoption and trustworthiness. Our study underlines the potential of PRV features in addressing some of these limitations. It was found that using morphological features from the PPG alongside PRV features extracted from this signal allows for a relatively good performance in BP estimation. The model with morphological features alone outperformed the model with pulse rate variability features, but the best performance was obtained using the combined set of features (RMSE: 5.71 mmHg). Although further studies with more representative populations and in more practical settings are necessary, this initial results indicate the capability of PPG and PRV-based features for the estimation of BP in a continuous manner, which could then be included in wearable and everyday devices for the monitoring of BP information.

CRedit authorship contribution statement

Elisa Mejía-Mejía: Conceptualization, Formal analysis, Methodology, Validation, Visualization, Writing – original draft, Reviewed, Revised the manuscript. **Karthik Budidha:** Carried experiments, Collected the data, Funding acquisition, Resources, Reviewed, Revised the manuscript. **Panayiotis A. Kyriacou:** Funding acquisition, Resources, Reviewed, Revised the manuscript. **Mohammad Mamouei:** Conceptualization, Formal analysis, Funding acquisition, Project administration, Resources, Supervision, Validation, Visualization, Reviewed, Revised the manuscript.

Declaration of competing interest

The authors declare that they have no known competing financial interests or personal relationships that could have appeared to influence the work reported in this paper.

Acknowledgment

The work is funded internally by Pleth AILytics ltd.

Appendix A. Supplementary data

Supplementary material related to this article can be found online at <https://doi.org/10.1016/j.bspc.2022.103968>.

References

- [1] What is blood pressure, 2019, Online <https://www.nhs.uk/common-health-questions/lifestyle/what-is-blood-pressure/>.
- [2] S.I. Fox, *Human Physiology*, 14 ed., McGraw Hill, New York, NY, 2016.
- [3] C. El-Hajj, P.A. Kyriacou, A review of machine learning techniques in photoplethysmography for the non-invasive cuff-less measurement of blood pressure, *Biomed. Signal Process Control* 58 (2020) 101870, <http://dx.doi.org/10.1016/j.bspc.2020.101870>.
- [4] C. El-Hajj, P.A. Kyriacou, Deep learning models for cuffless blood pressure monitoring from PPG signals using attention mechanism, *Biomed. Signal Process Control* 65 (2021) 102301, <http://dx.doi.org/10.1016/j.bspc.2020.102301>.
- [5] Understanding blood pressure readings, 2021, Online <https://www.heart.org/en/health-topics/high-blood-pressure/understanding-blood-pressure-readings>.

- [6] R. Mukkamala, J.-O. Hahn, O.T. Inan, L.K. Mestha, C.S. Kim, H. Töreyn, S. Kyal, Towards ubiquitous blood pressure monitoring via pulse transit time: Theory and practice, *IEEE Trans. Biomed. Eng.* 62 (8) (2015) 1879–1901, <http://dx.doi.org/10.1109/TBME.2015.2441951>.
- [7] M. Radha, K. de Groot, N. Rajani, C.C.P. Wong, N. Kobold, V. Vos, P. Fonseca, N. Mastellos, P.A. Wark, N. Velthoven, R. Haakma, R.M. Aarts, Estimating blood pressure trends and the nocturnal dip from photoplethysmography, *Physiol. Meas.* 40 (2019) 025006, <http://dx.doi.org/10.1088/1361-6579/ab030e>.
- [8] G. Chan, R. Cooper, M. Hosanee, K. Welykholowa, P.A. Kyriacou, D. Zheng, J. Allen, D. Abbott, N.H. Lovell, R. Fletcher, M. Elgendi, Multi-site photoplethysmography technology for blood pressure assessment: Challenges and recommendations, *J. Clin. Med.* 8 (11) (2019) 1827, <http://dx.doi.org/10.3390/jcm8111827>.
- [9] M. Hosanee, G. Chan, K. Welykholowa, R. Cooper, P.A. Kyriacou, D. Zheng, J. Allen, D. Abbott, C. Menon, N.H. Lovell, H. Newton, W.S. Chan, K. Lim, R. Fletcher, R. Ward, M. Elgendi, Cuffless single-site photoplethysmography for blood pressure monitoring, *J. Clin. Med.* 9 (3) (2020) 723, <http://dx.doi.org/10.3390/jcm9030723>.
- [10] K. Welykholowa, M. Hosanee, G. Chan, R. Cooper, P.A. Kyriacou, D. Zheng, J. Allen, D. Abbott, C. Menon, N.H. Lovell, N. Howard, W.S. Chan, K. Lim, R. Fletcher, R. Ward, M. Elgendi, Multimodal photoplethysmography-based approaches for improved detection of hypertension, *J. Clin. Med.* 9 (4) (2020) 1203, <http://dx.doi.org/10.3390/jcm9041203>.
- [11] M. Elgendi, R. Fletcher, Y. Liang, N. Howard, N.H. Lovell, D. Abbott, K. Lim, R. Ward, The use of photoplethysmography for assessing hypertension, *Npj Digit. Med.* 2 (2019) 60, <http://dx.doi.org/10.1038/s41746-019-0136-7>.
- [12] P.A. Kyriacou, Introduction to photoplethysmography, in: P. Kyriacou, J. Allen (Eds.), *Photoplethysmography: Technology, Signal Analysis, and Applications*, Elsevier, London, UK, 2021, pp. 69–145.
- [13] E. Mejía-Mejía, J.M. May, R. Torres, P.A. Kyriacou, Pulse rate variability in cardiovascular health: a review on its applications and relationship with heart rate variability, *Physiol. Meas.* 41 (2020) 07TR01, <http://dx.doi.org/10.1088/1361-6579/ab998c>.
- [14] E. Mejía-Mejía, K. Budidha, T.Y. Abay, J.M. May, P.A. Kyriacou, Heart rate variability (HRV) and pulse rate variability (PRV) for the assessment of autonomic responses, *Front. Physiol.* 11 (2020) 779, <http://dx.doi.org/10.3389/fphys.2020.00779>.
- [15] E. Mejía-Mejía, J.M. May, M. Elgendi, P.A. Kyriacou, Classification of blood pressure in critically ill patients using photoplethysmography and machine learning, *Comput. Meth. Prog. Bio.* 208 (2021) 106222, <http://dx.doi.org/10.1016/j.cmpb.2021.106222>.
- [16] E. Mejía-Mejía, J.M. May, M. Elgendi, P.A. Kyriacou, Differential effects of the blood pressure state on pulse rate variability and heart rate variability in critically ill patients, *Npj Digit. Med.* 4 (2021) 82, <http://dx.doi.org/10.1038/s41746-021-00447-y>.
- [17] A. Gaurav, M. Maheedhar, V.N. Tiwari, R. Narayanan, Cuff-less PPG based continuous blood pressure monitoring - a smartphone based approach, in: *Proc Annu Int Conf IEEE Eng Med Biol Soc*, 2016, pp. 607–610, <http://dx.doi.org/10.1109/EMBC.2016.7590775>.
- [18] M.W.K. Fong, E.Y.K. Ng, K.E.Z. Jian, T.J. Hong, SVR ensemble-based continuous blood pressure prediction using multi-channel photoplethysmogram, *Comput. Biol. Med.* 113 (2019) 103392, <http://dx.doi.org/10.1016/j.compbiomed.2019.103392>.
- [19] A.E.W. Johnson, T.J. Pollard, L. Shen, L.W.H. Lehman, M. Feng, M. Ghassemi, B. Moody, P. Szolovits, L.A. Celi, R.G. Mark, MIMIC-III, A freely accessible critical care database, *Sci. Data* 3 (2016) 160035, <http://dx.doi.org/10.1038/sdata.2016.35>.
- [20] A.L. Goldberger, L.A.N. Amaral, L. Glass, J.M. Hausdorff, P.C. Ivanov, R.G. Mark, J.E. Mietus, G.B. Moody, C.K. Peng, H.E. Stanley, PhysioBank, PhysioToolkit, And PhysioNet: Components of a new research resource for complex physiologic signals, *Circulation* 101 (23) (2000) e215–e220, <http://dx.doi.org/10.1161/01.cir.101.23.e215>.
- [21] G. Slapničar, M. Luštrek, Continuous blood pressure estimation from PPG signal, *Informatica (Slovenia)* 42 (2018) 33–42.
- [22] G. Slapničar, N. Mlakar, M. Luštrek, Blood pressure estimation from photoplethysmogram using a spectro-temporal deep neural network, *Sensors (Basel)* 19 (15) (2019) 3420, <http://dx.doi.org/10.3390/s19153420>.
- [23] J. Leitner, P.H. Chiang, S. Dey, Personalized blood pressure estimation using photoplethysmography and wavelet decomposition, in: 2019 IEEE International Conference on E-Health Networking, Application and Services, HealthCom, 2019, pp. 1–6, <http://dx.doi.org/10.1109/HealthCom46333.2019.9009587>.
- [24] T. Athaya, S. Choi, An estimation method of continuous non-invasive arterial blood pressure waveform using photoplethysmography: A U-net architecture-based approach, *Sensors (Basel)* 21 (5) (2021) 1867, <http://dx.doi.org/10.3390/s21051867>.
- [25] N. Aguirre, E. Grall-Maš, L.J. Cymberknop, R.L. Armentano, Blood pressure morphology assessment from photoplethysmogram and demographic information using deep learning with attention mechanism, *Sensors (Basel)* 21 (6) (2021) 2167, <http://dx.doi.org/10.3390/s21062167>.
- [26] CNAP Blood pressure, 2021, Online <https://www.cnsystems.com/technology/cnap-blood-pressure/>.
- [27] B.N. Li, M.C. Dong, M.I. Vai, On an automatic delineator for arterial blood pressure waveforms, *Biomed. Signal Process Control* 5 (2010) 76–81, <http://dx.doi.org/10.1016/j.bspc.2009.06.002>.
- [28] M. Elgendi, I. Norton, M. Brearley, D. Abbott, D. Schuurmans, Systolic peak detection in acceleration photoplethysmograms measured from emergency responders in tropical conditions, *PLoS One* 8 (10) (2013) e76585, <http://dx.doi.org/10.1371/journal.pone.0076585>.
- [29] R. Wilcox, The regression smoother LOWESS: A confidence band that allows heteroscedasticity and has some specified simultaneous probability coverage, *J. Mod. Appl. Stat. Methods* 16 (2017) 29–38, <http://dx.doi.org/10.22237/jmasm/1509494580>.
- [30] E. Gil, M. Orini, R. Bailón, J.M. Vergara, L. Mainardi, P. Laguna, Photoplethysmography pulse rate variability as a surrogate measurement of heart rate variability during non-stationary conditions, *Physiol. Meas.* 31 (9) (2010) 1271–1290, <http://dx.doi.org/10.1088/0967-3334/31/9/015>.
- [31] I. Constant, D. Laude, I. Murat, J.L. Elghozi, Pulse rate variability is not a surrogate for heart rate variability, *Clin. Sci.* 97 (1999) 391–397.
- [32] E. Mejía-Mejía, J. Allen, K. Budidha, C. El-Hajj, P.A. Kyriacou, P.H. Charlton, Photoplethysmography signal processing and synthesis, in: P.A. Kyriacou, J. Allen (Eds.), *Photoplethysmography: Technology, Signal Analysis and Applications*, Elsevier, 2021, pp. 69–145.
- [33] E. Mejía-Mejía, J.M. May, P.A. Kyriacou, Effects of using different algorithms and fiducial points for the detection of interbeat intervals, and different sampling rates on the assessment of pulse rate variability from photoplethysmography, *Comput. Methods Programs Biomed.* 218 (2022) 106724, <http://dx.doi.org/10.1016/j.cmpb.2022.106724>.
- [34] E. Mejía-Mejía, J.M. May, P.A. Kyriacou, Effect of filtering of photoplethysmography signals in pulse rate variability analysis, in: *Annu. Int. Conf. IEEE Eng. Med. Biol. Soc.*, 2021, pp. 5500–5503, <http://dx.doi.org/10.1109/EMBC46164.2021.9629521>.
- [35] M. Proença, G. Bonnier, D. Ferrario, C. Verjus, M. Lemay, PPG-based blood pressure monitoring by pulse wave analysis: Calibration parameters are stable for three months, in: *Annu. Int. Conf. IEEE Eng. Med. Biol. Soc.*, 2019, pp. 5560–5563, <http://dx.doi.org/10.1109/EMBC.2019.8857740>.